scientific reports

Check for updates

OPEN

The development of the soderberg electrolyzer electromagnetic field's state monitoring system

Ilyushin Yury & Alexander Martirosyan✉

This study is devoted to improving the economic efficiency of the cell, due to the field of the generated electromagnetic field's accurate diagnostics. To solve this problem, the authors had developed a hardware-software complex for electromagnetic field diagnostics. This complex includes a measurement device and a software package for data collection and analysis. On the laboratory prototype of the aluminum electrolysis complex, a study was carried out on the formation and structure of the electromagnetic field. A number of experiments have been carried out showing the degree of formation of the electromagnetic field by the anode, the relationship of electromagnetic fields in the inter-anode space has been shown. Based on the results of the studies, conclusions were drawn about the possibility of diagnosing the current state of the anode, determining the direction of rotation of aluminum in the electrolytic cell and estimating the life of the anode and its burnout time.

In November 2022, the United Nations announced that the world's population had crossed the threshold of 8 billion people[1]. Constantly growing market needs of the vehicles, consumer goods, packaging, construction, packaging materials, etc. needs the increasing of the burden on the metallurgical industry. The volume of the most used metals extraction (lead, aluminum, zinc, etc.) is no longer enough to meet all the needs of the industry and the market. The review of BCS analysts notes that the shortage of aluminum in the world will remain a key factor in supporting metal prices and may lead to their increase[2,3]. According to them, in the third quarter of 2022, the deficit of aluminum in the world amounted to 1.1 million tons[4]. The average selling price of aluminum in the first half of 2022 was USD 3,365/t (+47.1% YOY), supported by an increase in the average price on the London Metal Exchange taking into account the quotation period (LME QP) 1 (+45, 1% YoY, up to $3,023/t). At the same time, aluminum prices increased significantly in 1Q 2022, reaching USD 3,985. The cost of aluminum production in the first half of 2022 increased by 33.2% to USD 2,028 per ton (compared to USD 1,523 US dollars per tonne in the first half of 2021) due to increased costs for alumina, other raw materials and materials, as well as logistics[5]. An important factor in the pricing of primary aluminum is the efficiency of aluminum production. According to metallurgical companies, the cost of primary aluminum is growing by 5–10 percent annually. This is mainly due to the increase in the price of electricity, which is the most important and most energy-intensive resource (up to 65% of the cost of primary aluminum). Thus, the analysis of the technological process of obtaining primary aluminum, the identification of the most energy-consuming factors and their optimization will significantly reduce the cost of the final product.

Methods

Description of the technological process

Modern industrial production of aluminum is based on the electrolytic decomposition of alumina (Al_2O_3) in the melt of cryolite salts (3NaF·AlF3). This production technology can be provided by several types of electrolyzers. Prebaked anode (BA) cells operate at over 320 kA, and prototype designs over 400 kA, and 500 kA designs are reportedly under development. The productivity of modern electrolyzers reaches 2500 kg per day[6].

The cathode device of the ensouled anode cell (EAC) electrolyzer is a powerful metal cathode casing, in which a carbon conductive bath about 50 cm deep is located, isolated from the casing by a refractory and heat-insulating lining. Liquid aluminum accumulates at the bottom of the bath shaft, and an electrolyte layer is located above it, in which the anode is immersed.

The anode device consists of carbon anode blocks arranged in two rows. The current is supplied to them through an anode rod attached to the anode bus. The escaping anode gases are collected in the gas collection casing and sucked off by smoke exhausters to the gas treatment plants.

Saint Petersburg Mining University, Saint Petersburg, Russia 199106. ✉email: martirosyan_av@pers.spmi.ru

Electrolyzers with Soderberg anodes (ESA) differ from EAC electrolyzers in the design of the anode. Prebaked coal blocks are installed on the EAC electrolyzers, and on the ESA electrolyzers, the anode is formed from the carbonaceous mass directly on the electrolyzer under the action of the released heat. The designs of the cathode device for electrolyzers of all types do not have significant differences.

Theoretically, it is convenient to consider the process of aluminum electrolysis on the diagram of the simplest electrolytic installation (Fig. 1).

An anode is located in the upper part of the cell, partially immersed in the molten electrolyte 3. When the positive pole of the DC source is connected to the anode and the negative pole to the graphite plate, an electric current will flow through the cell, which will cause chemical changes in the electrolyte. This process is called electrolysis. During the decomposition of alumina, aluminum is released at the cathode, and oxygen is released at the anode, which, oxidizing the carbon anode, leads to the formation of CO and CO_2.

In order for an electric current to flow through a cell, a certain voltage must be applied to it. If this voltage is greater than the alumina decomposition voltage Ep, then the electrolysis process will begin. If the applied voltage is less than Ep, no current will flow through the cell.

With an inert anode (platinum, ferrites, etc.), the decomposition of alumina will occur according to the reaction:

$$Al_2O_3 \leftrightarrow 2Al + 1.5O_2 \text{ while } E_p = 2.19 \text{ V } [6, 8, 9].$$

On the carbon anode, which is equipped with all operating electrolyzers, two reactions are possible—with the formation of CO2 and with the formation of CO:

$$2Al_2O_3 + 3C \leftrightarrow 4Al + 3CO_2 \text{ while Ep } = 1.167 \text{ V};$$

$$Al_2O_3 + 3C \leftrightarrow 2Al + 3CO \text{ while } E_p = 1.034 \text{ V } [7, 24, 25].$$

That is, with a carbon anode, the voltage of alumina decomposition is less than with an inert anode, since part of the energy necessary for the decomposition of alumina is released during the oxidation of the carbon anode. Therefore, the minimum voltage at which the electrolysis process begins is commonly called the back EMF.

Measurements carried out on industrial electrolyzers showed that back EMF is in the range of 1.4–1.8 V, and its value is influenced by the anode current density, the chemical activity of the carbon anode, the process temperature, and a number of other factors[3]. Consider the main parameters of the electrolysis process.

The amount of aluminum Q_o (kg), which theoretically can be obtained in the electrolysis process for a certain period of time t (h), is determined by Faraday's law $Q_o = k \cdot I \cdot t$, where k is the electrochemical equivalent of aluminum, equal to 0.3354 g/A·h or kg/kA·h; I is the current strength, kA.

In practice, due to the oxidation reactions of the obtained aluminum in the electrolyte during its interaction with the anode gases, as well as due to some current leakage, the actual amount of aluminum obtained Q_a is always less than the theoretically possible value. The ratio of the practically obtained metal Q_a to the theoretically possible Q_o is called the current output η and is expressed as a percentage or fractions of a unit:

$$\eta = \frac{Q_o}{Q_a}$$

Then

$$Q_a = k \cdot I \cdot t \cdot \eta.$$

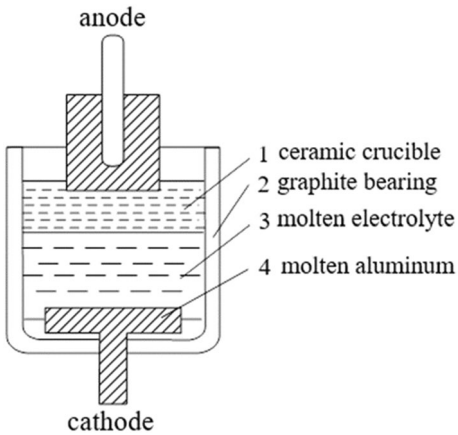

Figure 1. Diagram of an electrolytic cell.

The current output characterizes the efficiency of current use and is the most important technical indicator of the electrolysis process. On modern electrolyzers, the value of η is in the range from 0.85 to 0.95. The daily capacity of the Q_{24} cell (which in practice is called "bath-day") is equal to

$$Q_{24} = k \cdot I \cdot t \cdot \eta = 0,3354 \cdot 24 \cdot I \cdot \eta = 8,05 \cdot I \cdot \eta.$$

Specific electricity consumption

A very important indicator of the efficiency of electrolysis technology is the specific consumption of direct current electricity per unit of aluminum produced w (kW h / t), that is, the ratio of the energy expended W (kW h) to the amount of aluminum produced Q_a (t). The amount of energy spent W at direct current is determined by the formula

$$W = I \cdot U_m$$

where I is the current strength, kA; U_m is the average voltage on the cell, V; t is the duration of the electrolysis process, h.

The specific consumption of direct current electricity for the production of 1 ton of aluminum is calculated by the formula:

$$W = \frac{W}{O} = \frac{I \cdot U_m \cdot t}{k \cdot I \cdot t \cdot \eta} = \frac{U_m}{k \cdot \eta}$$

The specific power consumption at operating electrolyzers is 13.5–16 thousand kWh/t. In practice, the reciprocal of the specific electricity consumption is often used—energy efficiency (η_e), this is the aluminum yield in grams per kWh consumed:

$$\eta_e = \frac{1}{\eta} = \frac{k \cdot \eta}{U_m}$$

When converting alternating current to direct current, power losses are formed in the busbar, as well as in transformers and rectifiers of converter units. The conversion factor (efficiency factor) of silicon-converting substations (SCS) of aluminum plants is an integral indicator that characterizes the amount of electrical energy loss for converting industrial frequency alternating current into rectified current. The coefficient is determined by calculation at the design stage of the object. In general, it depends on the following parameters:

1. Gearbox equipment layout, voltage class, rectified current value. At AZ ADV, substations with a rectified voltage of 450, 600, 950, 1000 and 1500 V are in operation. The magnitude of the rectified current is from 140 to 313 kA.
2. The number of rectifier units installed at one SCS, their technical characteristics.
3. Cross-sections and lengths of current-carrying conductors of the power supply circuit (losses are directly proportional to the square of the current multiplied by the resistance of the conductor).
4. Accuracy class and type of rectified current measurement systems (measurement system IS-225, monoblock high current meter PIPT-180, FOCS-350).
5. Repair modes of the equipment's operation of the SCS and GPP, the withdrawal of individual elements of the equipment from work during the modernization of facilities.
6. Temperature regimes of outdoor air.

The conversion factor is an important indicator characterizing the losses of the SCS, which is controlled, calculated and taken into account on a daily basis. Changing the conversion factor makes it possible to improve the accuracy of determining the state of the rectified and commercial current measurement systems, changing the power supply circuits of the SCS during the day, and the operation of the equipment in repair mode. The maintenance of technological and energy parameters (current) of the electrolysis series is carried out by switching the tap changer stages of the transformers or by changing the current saturation chokes. In this case, the conversion factor changes. Which allows you to calculate the weighted average daily.

With long-term operation of the equipment and a gradual change in their parameters (equipment aging), the losses increase, while the conversion factor decreases.

These conversion losses are determined by calculation, and the consumption of energy for the own needs of the converter substation is added to them. The ratio of direct current energy W to the received alternating current energy W_{AC} is called the conversion factor EF (efficiency factor):

$$EF = \frac{W}{W_{AC}}$$

At modern plants, the EF value is in the range of 0.96–0.98. Conversion losses also depend on the type of rectifiers and transformers used, they decrease with increasing current strength and, especially, with increasing number of operating electrolyzers in a series. The dominant part of the energy losses occurs in the transformers of the rectifier units. Energy losses in transformers consist of losses in the transformer windings ("copper losses") and iron remagnetization losses ("iron losses"). Losses in copper reach 80–85% of the total energy losses in transformers and do not depend on the voltage value. Losses in the iron of transformers are relatively small and increase to a lesser extent with increasing voltage than losses in copper with an adequate increase in current strength.

Thus, a number of key conclusions can be drawn:

1. Electric current (electromagnetic field) is the main factor shaping the process of electrolysis and production of aluminum.
2. An electrolyser, as a complex technical device, has many technically complex elements where electrical energy losses occur, most of which can be traced only by the consequences they have on the technological process.

These conclusions, to one degree or another, were considered by scientists from many countries and pointed to the features of this technological process as an object of control. It is proposed to consider some of them.

The state of knowledge of the problem

The first work on the interaction of the electromagnetic field dates back to 1819, in which the Danish physicist H.K. phenomena are interconnected. In 1832, Faraday established that the mass of the substance released on the electrode is directly proportional to the electric charge that has passed through the electrolyte. In 1886, Martin Hall creates the first electrolyzer. After that, many scientists around the world began to engage in research in the field of electrolysis, and the production of electrical energy in general. The main works in this area belong to Borisoglebsky Yu.V., Begunov A.I., Levin M.V., Arkhipov G.V., Vetyukov M.M., Zelberg B.I., Lokshin R.G., Kuptsov A. N., Demykin P.A., Kontsur E.P., Mintsis M.Ya., Mann V.Kh., Piskazhova T.V., Skornyakov V.I., Chalykh V.I., Polyakov P.V ., Berezin A.I., Nikolaev I.V. Platonov V.V., and many others. Research in this area abroad is carried out by a number of scientists: A. Zarouni, L. Mishra, J. Thonstad, M. Dupuis, V. Bojarevics, and others. Boikov A. in his works, for example[7,8], shows the importance of analyzing the cell as a complex system, taking into account multiple input and output parameters. And in[9] he uses a neural network to analyze the structure of the quality of the metal. The work[10] considers the energy efficiency of the units and their impact on the final cost of the manufactured product. The economic assessment of general costs[11] and the assessment of environmental pollution[12] are rather difficult to assess. Therefore, these factors will not be assessed in the present study.

A special role should be given to the work[13], which presents a three-dimensional non-stationary model of a 600 kA electrolytic cell. and made a detailed description of the process of electrolysis occurring in the cell. However, this mathematical model has a number of disadvantages associated with a rather large discretization of the model[14]. In order to increase the accuracy of calculations of electromagnetic fields of electrolyzers, Chinese scientists[15] propose to use a genetic neural network. Similar conclusions were reached in works[16–21]. In general, field monitoring issues are dealt with in the context of the study of technological processes as objects of control. This approach provides high visibility, but rather low measurement accuracy. To improve the accuracy of the study, various mathematical tools are used, for example, in[22], a new model of an uncontrolled neural network, called a network with slow functions (SFNet), is proposed for monitoring dynamic processes. Thus, the main direction of increasing the measurement accuracy is the development of new methods and models for processing the obtained models[23]. Another direction in this area is the experimental direction. The essence of this direction is to conduct a huge number of experiments and build regression models based on it[24,25]. These models are highly accurate at a given time, but are completely inapplicable to the analysis of dynamic systems with constantly changing input, internal and output parameters[26,27]. If we analyze a complex but relatively stable process, for example[28], this approach takes place, but it is not without drawbacks, for example, in such models it is quite difficult to determine which parameters are responsible for the environment[29], the technological process, etc. conditions when the rate of aluminum production is 6–8 h, this approach is not applicable. When analyzing such systems, it is necessary to take into account not only factors, but also the geometric parameters of the object. Such an approach in systems theory is called spatially distributed. This approach was first proposed by Pershin I.M.[29] and continued in the works of his students[30,31]. European scientists[32,33] also take into account spatial components when automating technological processes. Including when studying the issues of deformation of aluminum products[34–42]. This approach makes it possible to accurately determine the parameters of the technological process[43,44]. Within the framework of this study, it is proposed to consider an experiment, as a result of which, using an independently developed device, models of a dynamically changing electromagnetic field can be obtained.

Speaking about the methodological component, it is important to mention, that in modern economic conditions, the development of a software and hardware complex should be carried out under strict weight and size conditions while minimizing production costs. As was shown in works[45–48], taking into account the limitations[49–53], the economic assessment of the work consists not only of internal and external factors, but also of the market's current state. Most parameters of the current state are associated with the demand of the goods and services on the market. Aluminum in this context is one of the main engines in the automobile and aircraft industries. In the context of transportation of oil, gas, biodiesel[54] and other components that are directly related to the cost of transportation, a number of economic factors influencing metallurgy can be identified:

1. Prices of metal resources: Prices of steel, iron, aluminum and other metals have a direct impact on metallurgical production. Increasing prices for metals can increase the cost of production and reduce the demand for metallurgical products[1–3,10,16,45–49,55,56].
2. Demand for metallurgical products: economic growth and the construction industry can lead to an increase in demand for metallurgical products, while a recession in the economy can reduce demand[2–5,7,19,22,28–30,45–49,57–62].
3. Innovation and technological progress: the introduction of new technologies and processes can increase the productivity and efficiency of metallurgical production, which can have a positive impact on its development[2–5,7,19,22,28–30,57,63–65].

4. Government policy and regulation: Government regulatory measures such as taxes, legislation and customs duties can influence the stimulation or restriction of metallurgical production[2–5,7,11,12,14,23–25,27,38–44].
5. .International competition: Metallurgical production is a global market, and competition from other countries can put pressure on local producers[1–5,7,54–56,59–70].

Thus, within the framework of this study, the development of a software and hardware complex has strict restrictions in terms of weight and size. Since the developed product is tasked with confirming the fundamental possibility of such diagnostics, and not with industrial operation, a number of requirements can be neglected.

It should also be noted that within the framework of this study, systems analysis methods will be used aimed at increasing the accuracy of the results. To carry out a system analysis of aluminum electrolysis, the following methods can be most often used:

1. Flow Diagram: This method consists of constructing a diagram that shows the flow of materials, energy and information in an aluminum electrolysis system. A flow diagram helps to identify the main components of the system and determine the flow of resources between them[11,12,14–24,28–42,57,65,71–76].
2. System model. The system model can be mathematical, physical or computer. It allows you to study the influence of various variables on the operation of the system and optimize the electrolysis process[18–22,28–35,57,77–79].
3. Function analysis. This method consists of determining the functions performed by the various elements of the aluminum electrolysis system. Function analysis helps to understand how the system works and what problems or improvements may exist[4,5,7,8,79–85].
4. Analysis of the system structure. This method involves studying the relationships between the various elements of an aluminum electrolysis system. Structure analysis helps determine which elements are most important for the operation of the system and how a change in one element can affect other elements[19,42,82–86].
5. Stability analysis. This method involves studying the stability of an aluminum electrolysis system. Stability analysis helps to understand how a system reacts to changes in external conditions and what measures can be taken to prevent failures or accidents[34–36,86–91].

These systems analysis techniques can be applied to study various aspects of an aluminum electrolysis system and optimize the operation of the process. This work involves data collection and physical monitoring. After obtaining a range of initial data, the results obtained can be processed by any of the above proposed methods. This versatility is achieved by using a spatially distributed sensor. It makes it possible to construct a temperature dependence not from one single measurement location, but from all areas of the research object. Similar works were considered in[92–106] but were applied to other objects. Thus, the logicality of the chosen research path was confirmed.

Results

The development of the program apparatus complex for the electric field measuring

The main device for measuring the electromagnetic field is the Hall sensor. The principle of operation of the sensor is based on the Hall effect and its initial voltage is directly proportional to the magnetic field strength. Analog sensors make it possible to obtain a differentiated value of the state of the electromagnetic field within the measured range. The A3144 sensor was selected for laboratory testing. To measure the uniformity of the electromagnetic field, the sensors must be located equidistant from each other. For this, a grid is formed, shown in Fig. 2.

The equilateral grid is a 5×5 sensor cube. Thus, there are 25 sensors in the layer, directed perpendicularly to the walls upwards. The sensors are located in hollow tubes that form the walls of the cube (Fig. 3).

Thus, an equilateral grid is formed consisting of four layers of 25 sensors each. Each sensor is connected to an 8-channel multiplexer, and then to the control microcontroller. Then 100 sensors are combined into a single

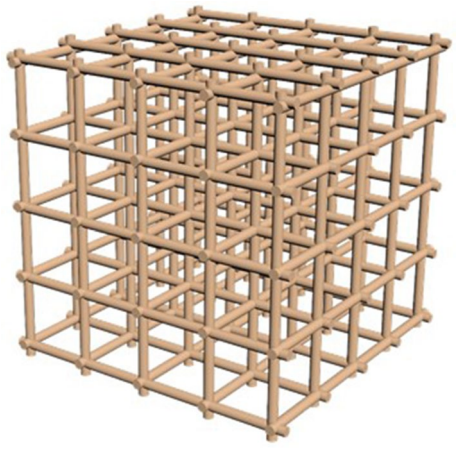

Figure 2. Equilateral grid of the measuring complex.

calculation system. For the convenience of building an electronic circuit, all power and ground buses are connected by single conductors. Thus, there is no overload of the current-carrying bars to each sensor. Data buses have an independent supply to the multiplexers. In general, the electronic circuit of each mounting layer looks like shown in Fig. 4.

The software part of the developed program apparatus complex (PAC) consists in the program code executed in C + + in the Arduini IDE. A feature of the developed program code is the absence of a multi-level connection with the I/O libraries. Since the main problem of sensors is the response time, and for such a large number of them, the delay time will be 6.4 s. The authors made a decision on parallel processing of data from sensors. The microcontroller allows you to process data from 4 channels simultaneously. By setting separators for the data stream received from the controller, we managed to reduce the response time to 1.6 s. A sketch that can be closed into a microcontroller that performs this function is presented below:

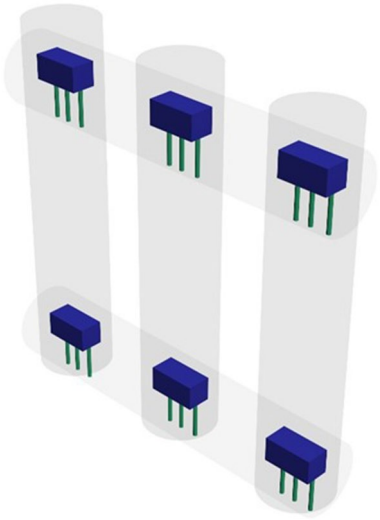

Figure 3. Location of sensors in hollow tubes forming a cube (fragment).

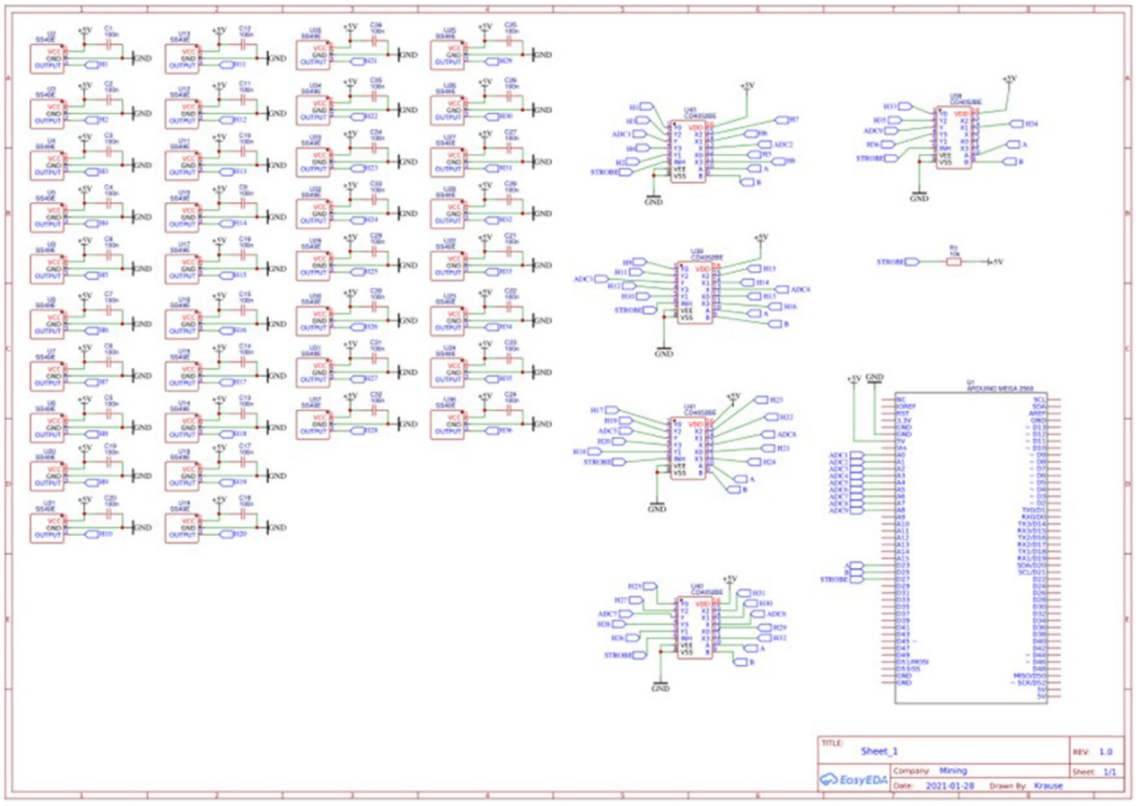

Figure 4. Scheme of connecting Hall sensors to the controller.

```
oid loop() {
 if (Serial.available() > 0)
{
 char in_data = Serial.read();
 if(in_data == '<'){
 for (int i = 0; i <= 15; i++){
 digitalWrite(S0,bitRead(i, 0));
 digitalWrite(S1,bitRead(i, 1));
 digitalWrite(S2,bitRead(i, 2));
 digitalWrite(S3,bitRead(i, 3));
 delay(50);
 Stroka = Stroka+ analogRead(SIG_A0)+" "+analogRead(SIG_A1) + " "+analogRead (SIG_A2) +" "+ analogRead(SIG_A3)+" "+
analogRead(SIG_A4)+ " "+ analogRead(SIG_A5) +" ";
 }
 Serial.println(Stroka);
 Stroka = "";
  } } }
```

The data rate is set to 9600 kilobits per second. The total amount of input data does not exceed 6000 kilobits per second.

A software module has been developed to process the received data. The module was developed in Borland Developer Studio 2006[107] in the Delphi programming language. COM + libraries[108] are used to work with external devices. After connecting the specified libraries, the library model looks like this:

```
Winapi.Windows, Winapi.Messages, System.SysUtils, System.Variants, System.Classes, Vcl.Graphics,
Vcl.Controls, Vcl.Forms, Vcl.Dialogs, CPDrv, Vcl.ExtCtrls, Vcl.StdCtrls,
Vcl.Menus, SDL_plot3d, Vcl.ComCtrls, Vcl.Buttons, SDL_Colsel, SDL_sdlbase;
```

The program code fragment that loads data from COM into the program looks like this:

```
procedure TForm2.N4Click(Sender: TObject);
 var
 rez : TModalResult;
begin
 CommPortDriver1.PortName:='\\.\'+Start.Form1.ComboBox1.Text;
 CommPortDriver1.BaudRateValue:=9600;
 CommPortDriver1.InBufSize:=4096;
 CommPortDriver1.InputTimeout:=100;
 CommPortDriver1.OutBufSize:=4096;
 CommPortDriver1.OutputTimeout:=100;
 CommPortDriver1.DataBits:=db8BITS;
 CommPortDriver1.StopBits:=sb1BITS;
 CommPortDriver1.Connect;
if CommPortDriver1.Connect = true then
 begin
  sleep(2500);
  CommPortDriver1.SendString('<');
 end
 else
 MessageBox(Handle, Error!', 'Статус порта', 0);
 end;
```

The data is read in a line of 500 characters and with the fixation of the universal separator. Allowing you to identify the boundaries of the data of one sensor from another. In this case, streaming data can easily be represented as a two-column table. In the first column, which indicates the identification number of the sensor (in our case, these are the coordinates of its position), and in the second column, the current readings of this sensor. A fragment of the program code that performs such processing is presented below.

```
Razdelitel_chisel := 1;
 While Razdelitel_chisel <> 97 do
 begin
 p:=pos(' ',Result);
 res[Razdelitel_chisel]:=copy(Result,1,p-1);
 delete(Result,1,p);
 if not(TryStrToFloat(res[Razdelitel_chisel],float)) then
 begin
  res[Razdelitel_chisel]:='0,00';
 end;
 Razdelitel_chisel:=Razdelitel_chisel+1;
 end;
 Result:=''; // сброс
 CommPortDriver1.SendString('<');
 For Xod:=1 to 96 do
 begin
 if StrToFloat(res[Xod]) < 500 then
 begin
 res[Xod]:=FloatToStr( 500-StrToFloat(res[Xod]) );
 end;
 if StrToFloat(res[Xod]) >= 500 then
 begin
 res[Xod]:=FloatToStr( StrToFloat(res[Xod])-500 );
 end;
 end;
```

After that, a formula for graphical display the layer values of the sensor is formed. The complete build code is shown below.

```
Plot3D001.GridMat.Elem[ii-1,jj-1] :=
(StrToFloat(res[1])-AverageResult) *exp(-0.40*(sqr(ii-(XRes / 1.10))+sqr(jj-(YRes / 1.10)))) +
(StrToFloat(res[2])-AverageResult) *exp(-0.40*(sqr(ii-(XRes / 1.37))+sqr(jj-(YRes / 1.10)))) +
(StrToFloat(res[3])-AverageResult) *exp(-0.40*(sqr(ii-(XRes / 1.85))+sqr(jj-(YRes / 1.10)))) +
(StrToFloat(res[4])-AverageResult) *exp(-0.40*(sqr(ii-(XRes / 2.80))+sqr(jj-(YRes / 1.10)))) +
(StrToFloat(res[5])-AverageResult) *exp(-0.40*(sqr(ii-(XRes / 5.90))+sqr(jj-(YRes / 1.10)))) +

 (StrToFloat(res[6])-AverageResult) *exp(-0.40*(sqr(ii-(XRes / 1.10))+sqr(jj-(YRes / 1.37)))) +
 (StrToFloat(res[7])-AverageResult) *exp(-0.40*(sqr(ii-(XRes / 1.37))+sqr(jj-(YRes / 1.37)))) +
 (StrToFloat(res[8])-AverageResult) *exp(-0.40*(sqr(ii-(XRes / 1.85))+sqr(jj-(YRes / 1.37)))) +
 (StrToFloat(res[9])-AverageResult) *exp(-0.40*(sqr(ii-(XRes / 2.80))+sqr(jj-(YRes / 1.37)))) +
 (StrToFloat(res[10])-AverageResult) *exp(-0.40*(sqr(ii-(XRes / 5.90))+sqr(jj-(YRes / 1.37)))) +

 (StrToFloat(res[11])-AverageResult) *exp(-0.40*(sqr(ii-(XRes / 1.10))+sqr(jj-(YRes / 1.85)))) +
 (StrToFloat(res[12])-AverageResult) *exp(-0.40*(sqr(ii-(XRes / 1.37))+sqr(jj-(YRes / 1.85)))) +
 (StrToFloat(res[13])-AverageResult) *exp(-0.40*(sqr(ii-(XRes / 1.85))+sqr(jj-(YRes / 1.85)))) +
 (StrToFloat(res[14])-AverageResult) *exp(-0.40*(sqr(ii-(XRes / 2.80))+sqr(jj-(YRes / 1.85)))) +
 (StrToFloat(res[15])-AverageResult) *exp(-0.40*(sqr(ii-(XRes / 5.90))+sqr(jj-(YRes / 1.85)))) +

 (StrToFloat(res[16])-AverageResult) *exp(-0.40*(sqr(ii-(XRes / 1.10))+sqr(jj-(YRes / 2.80)))) +
 (StrToFloat(res[17])-AverageResult) *exp(-0.40*(sqr(ii-(XRes / 1.37))+sqr(jj-(YRes / 2.80)))) +
 (StrToFloat(res[18])-AverageResult) *exp(-0.40*(sqr(ii-(XRes / 1.85))+sqr(jj-(YRes / 2.80)))) +
 (StrToFloat(res[19])-AverageResult) *exp(-0.40*(sqr(ii-(XRes / 2.80))+sqr(jj-(YRes / 2.80)))) +
 (StrToFloat(res[20])-AverageResult) *exp(-0.40*(sqr(ii-(XRes / 5.90))+sqr(jj-(YRes / 2.80)))) +

 (StrToFloat(res[21])-AverageResult) *exp(-0.40*(sqr(ii-(XRes / 1.10))+sqr(jj-(YRes / 5.90)))) +
 (StrToFloat(res[22])-AverageResult) *exp(-0.40*(sqr(ii-(XRes / 1.37))+sqr(jj-(YRes / 5.90)))) +
 (StrToFloat(res[23])-AverageResult) *exp(-0.40*(sqr(ii-(XRes / 1.85))+sqr(jj-(YRes / 5.90)))) +
 (StrToFloat(res[24])-AverageResult) *exp(-0.40*(sqr(ii-(XRes / 2.80))+sqr(jj-(YRes / 5.90)))) +
 (StrToFloat(res[25])-AverageResult) *exp(-0.40*(sqr(ii-(XRes / 5.90))+sqr(jj-(YRes / 5.90)))) ;
 Plot3D001.Refresh;
```

This formula represents five blocks of five lines. This was done for a more informative perception of the grid. If one of the sensors is connected to the wrong port by mistake, this can be easily corrected by correcting the

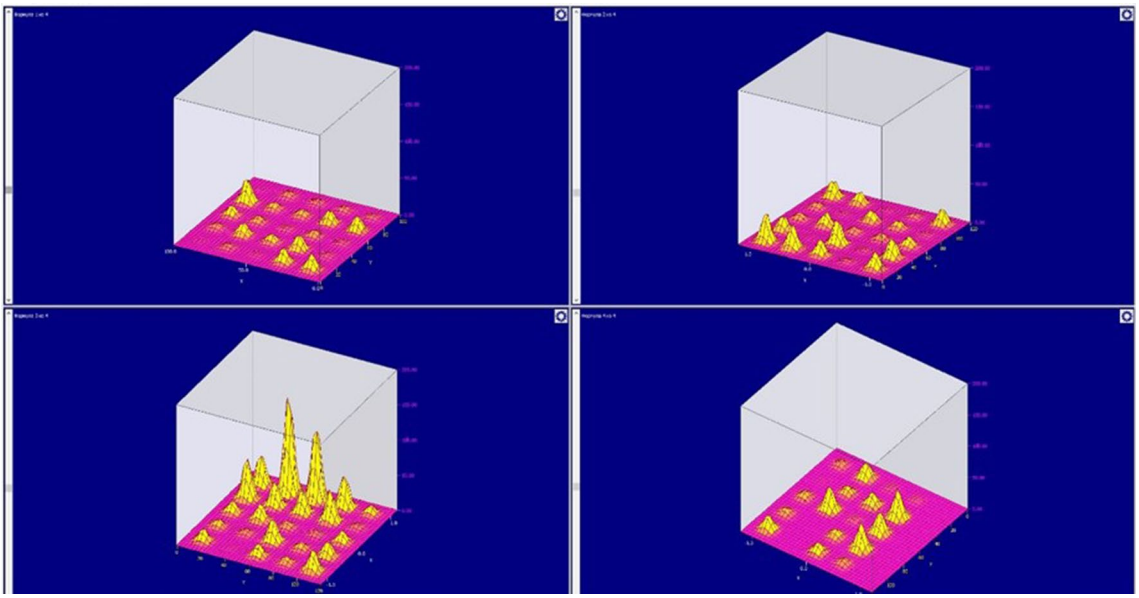

Figure 5. The interface of the developed PAC.

Parameter	Value
Bathtub dry weight	6600 kg
The mass of the filled bath	9300 kg
Bath dimensions (L × W × H)	4378 × 1108 × 1000 mm
Usable bath volume	2, 4 m^3/h
Pump capacity	2–3, 8 m^3/h
Electrode power supply	6 V, 2400 A
Control system:	Digital with smooth adjustment of voltage and current on the tires
Closed electrolyte circulation system	Closed electrolyte circulation system with safety overflow, one main circulation pump and one backup circulation pump
Power consumed from the mains 380	1.8 kW
Type of contact bar	Copper

Table 1. Technical characteristics of the object of study.

program code. It is also necessary to note the rigid binding of sensors to the coordinate grid. Such a binding will allow us to confirm the correctness of the preparation and collection of data from experiments conducted on the developed device. To display a graphical display, the freely distributed component SDL Component Suite[109] is used.

Figure 5 shows the main window of the developed software module. It is divided into four parts, each of which displays the state of the electromagnetic field in the corresponding layer. Accordingly, depending on the location of the object that forms the electromagnetic field, the sensor readings show a larger value (a unit of millivolts).

Thus, within the framework of the first part of the study, a software and hardware complex for measuring the electromagnetic field in laboratory conditions was developed. The task of this complex is to study the generated electromagnetic field and its dynamic characteristics. It is proposed to conduct a number of experimental studies aimed at the analysis of dynamically changing electromagnetic fields.

Experiments

As an object of study, we consider a working layout of a low-power electrolyzer. Technical characteristics of the electrolyzer are presented in Table 1.

Spatially distributed sensors of the electromagnetic field were installed in the area of the anode. The data obtained from the developed device is shown on the Fig. 6.

It is worth paying attention to the fact of the electromagnetic field uneven formation. This can be caused by two factors. The first is the error of each sensor. This shortcoming is eliminated by calibrating the sensors. The second drawback is the poor quality of the welded seams, which do not provide a uniform current flow to the anode. This drawback is eliminated by collecting statistical data and diagnosing current-carrying tires. At the initial stage of the electrolysis process, the anodes consume maximum power. This can be observed in Fig. 6.

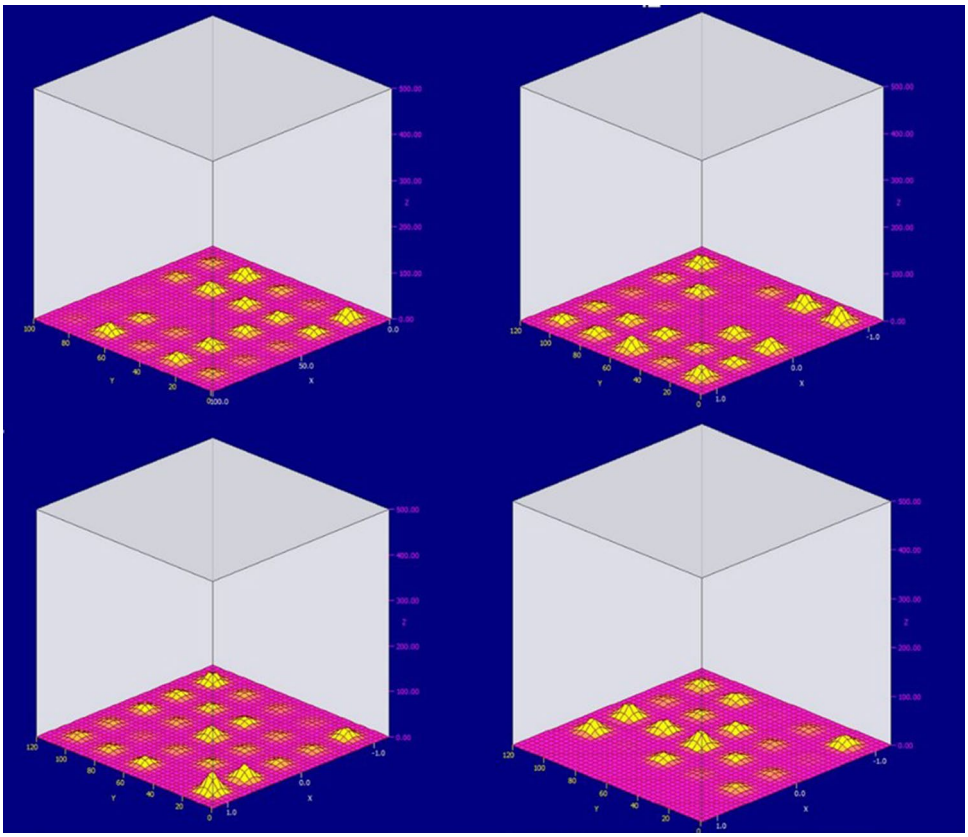

Figure 6. Graphs of the layer-by-layer propagation of the electromagnetic field formed by the first anode (on the graph on the x and z axes, spatial coordinates are indicated, along the y axis the values of the sensor readings are plotted).

From the presented figure, one can observe the maximum deviation in the first layer, moderate in the second, and in the third and subsequent minimum values. This is due to the distance of the anode object from the sensors.

It is also possible to observe a clear sphericity of the formulated electromagnetic field. It is proposed to consider the response of the electromagnetic field during measurements at the junction of two anodes. Figure 7 shows a graphical representation of the electromagnetic field generated by two adjacent anodes (only the first layer of sensors). Let's analyze the readings displayed on the graph.

1. It is necessary to pay attention to the inhomogeneity of the field formed by the anodes. This is due to their uneven burning. Such inhomogeneity causes a difference in the directions of current flow, which leads to the rotation of aluminum in the bath, and as a result, the deformation of the walls of the bath, the destruction of the lining, etc. Also, according to the shape of the electromagnetic field, it can be judged that the anode located on the left burns out in the middle, forming protruding edges on both sides. This will eventually chip off part of the anode and clog the bath.
2. At an equidistant point from two anodes, the value of the electromagnetic field is small. This may be due to insufficient working power of the cell, which can be caused by both uneven burnout of the anodes and initially incorrectly set power of the cell.
3. Extreme points far from the anode have zero readings. This also indicates insufficient power supplied to the anodes and their wear.

Identified defects may also indicate busbar defects and poor or excessive ground contact.

To identify this shortcoming, it is proposed to consider the fourth layer of sensors of the same area.

Figure 8 shows that the value of the electromagnetic field changes sign. Which is a sign of a violation of the integrity of the grounding system. It also indicates a low degree of isolation of the circulating currents.

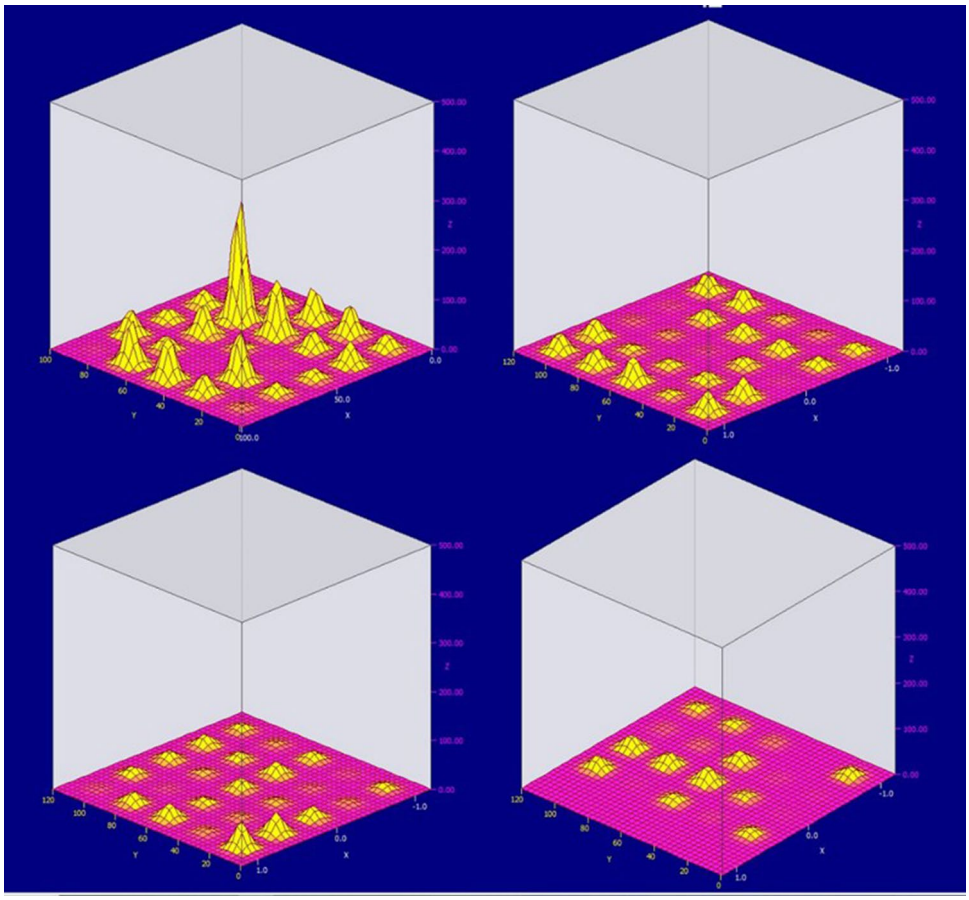

Figure 7. The value of the electromagnetic field between two anodes (1 layer of sensors).

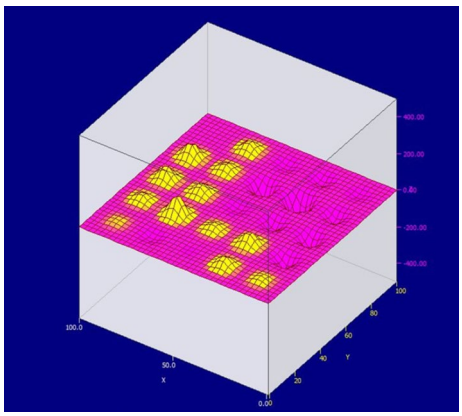

Figure 8. The value of the electromagnetic field between two anodes (4th layer of sensors).

Discussion

The industrial production of cheap aluminum is important for the industrialized countries economies growth. Within the framework of this study, a number of literary sources of economic, environmental and technical direction were analyzed, which made it possible to evaluate the efficiency of an aluminum production enterprise from an economic point of view. The analysis made it possible to determine the most costly component of the aluminum production process—energy consumption. The electrolyser, as the main consumer of electrical energy, plays the main role in it. The electrolysis process is not an energy efficient process due to the influence of a huge number of factors. As part of this study, the authors developed a device—a spatially distributed sensor of the electromagnetic field. With its help, a number of studies were carried out at a laboratory facility for the production of aluminum. Within the framework of this study, violations of the structural integrity of the electromagnetic

field were revealed. These violations could be detected only with the help of the developed device. Since at most enterprises there is a spot measurement of electromagnetic intensity. The developed software and hardware complex allows evaluating the entire structure of the electromagnetic field, pointing out specific shortcomings.

A special place in this study is occupied by the interpretation of the results obtained. It is important to note that the non-stationarity and inhomogeneity of the field makes it possible to point out a specific drawback of the cell element under study or its entirety.

Having obtained these results, shown in Fig. 6, it is possible to replace the burned-out anode at the moment when it burned out, and not when the time for its replacement has come according to the regulatory documentation. It should be noted that, depending on the rate of aluminum production, the anodes burn out unevenly, and in each cell the service life is determined based on either the service life or the difference in the current drop. The proposed hardware-software method will allow you to accurately determine the life of the anode.

The inhomogeneity of the field indicates eddy currents and rotation of the aluminum in the hearth. Using the results of this measurement, one can indirectly judge the direction of rotation. To provide measures the field's stabilizing and prevent rotation. In industrial conditions, this will significantly increase the operating time of the cell, as it makes it possible to eliminate one of the main factors of its destruction.

Using of the developed software and hardware complex will significantly expand the functionality of diagnostics of industrial electrolyzers. At the same time, a number of shortcomings of this device should be noted. The main one is accuracy. To ensure the given accuracy, it is necessary to use a large number of sensors. If there are not enough of them, the purity of discretization will be too large to determine specific shortcomings. And the use of sector diagnostics will not reflect the dynamics and can only be used for local measurement, which can be eliminated by increasing the number of sensors (measuring points), which will affect the final cost of the product. However, since the device is not disposable and is intended only for diagnostics, and not for continuous monitoring, the significance of this drawback is minimal.

At the same time, it is necessary to note the ways of the developed device further improvement. The works[110–122] indicate ways to increase the accuracy and industrial adaptation of the developed device. This direction will be the result of authors' further research.

Conclusion

In the context of the economic crisis and the deterioration of the environmental situation, production processes that combine the low cost of the product and its high quality are becoming increasingly important. It can be achieved only by creating an environmentally friendly and cost-effective production. The considered economic, environmental, state factors[123] affecting pricing show the need for a deep analysis of the factors affecting the product as the final product. For the technological process of aluminum production, this is electricity. Also the green energeticimprovement dimension can be considered as a possible implementation area[124]. Within the framework of this study, the authors developed a software and hardware complex for diagnosing the electromagnetic field of the electrolytic cell. A number of studies were carried out on a laboratory unit for the production of aluminum. It should be noted that based on the results of the work, a patent was issued for the invention "Device for diagnosing an electromagnetic field"[58]. Having demonstrated the possibilities of measuring and interpreting the results obtained, a direction was presented to increase the economic efficiency of the electrolytic cell.

Data availability

The datasets generated and/or analysed during the current study are available in the «SR Data» repository («Arduino» code for hardware, «Program» calculation code, «Result» additional result's data), (https://drive.google.com/drive/folders/1_d_m31sKwbeOaSHT-JqZuE8YtNKiWBwd?usp=sharing).

Received: 17 July 2023; Accepted: 12 January 2024
Published online: 12 February 2024

References

1. World population to reach 8 billion on 15 November 2022. https://www.un.org/en/desa/world-population-reach-8-billion-15-november-2022
2. Khaykin, M. & Toechkina, O. Service capital as a condition for the sustainable development of society. *Int. J. Technol.* https://doi.org/10.14716/IJTECH.V12I7.5360 (2021).
3. Khaikin, M., Shabalov, M., Ivanova, D. & Shapiro, N. A. Possible effects of economy digitalization processes on Russian mining industry from economic theory point of view. In *Advances in Raw Material Industries for Sustainable Development Goals*, 481–491 (2021).
4. Mingazov S. UC Rusal predicted a deficit of aluminum in 2022 up to 1.7 million tons.Forbes. https://www.forbes.ru/investicii/454457-rusal-predskazal-deficit-aluminia-v-2022-godu-do-1-7-mln-tonn
5. RUSAL announces interim results for the first half of 2022. Advis Agency. https://advis.ru/php/view_news_ajax.php?id=68F381D0-77CC-7C41-84B7-CD650444A02B
6. Philipson, H. The effect of thickness and compaction on the recovery of aluminium in recycling of foils in salt flux. (NTNU) Trondheim, Norway (2020).
7. Boikov, A. & Payor, V. The present issues of control automation for levitation metal melting. *Symmetry* **2022**, 14. https://doi.org/10.3390/sym14101968 (1968).
8. Vasilyeva, N. V. *et al.* Automated digitization of radial charts. *J. Min. Inst.* **247**(1), 82–87 (2021).
9. Boikov, A. *et al.* Synthetic data generation for steel defect detection and classification using deep learning. *Symmetry* **13**, 21100201542. https://doi.org/10.3390/sym13071176 (2021).
10. Shabalov, MYu. *et al.* The influence of technological changes in energy efficiency on the infrastructure deterioration in the energy sector. *Energy Reports* **7**, 2664–2680. https://doi.org/10.1016/j.egyr.2021.05.001 (2021).
11. Nikolaichuk, L. A., Malyshkov, G. B. & Sinkov, L. S. Analysis of economic evaluation methods of environmental damage at calculation of production efficiency in mining industry. *Int. J. Appl. Eng. Res.* **10**(12), 2551–2554 (2017).

12. Petrova, T. A , Rudzisha, E., Alekseenko, A. V., Bech. J. & Pashkevich M. A. Rehabilitation of disturbed lands with industrial wastewater sludge minerals. **12**, 376–376 (2022). https://doi.org/10.3390/min12030376.
13. Smolnikov, A. D. & Sharikov, Y. V. Simulation of the aluminum electrolysis process in a high-current electrolytic cell in modern software. *Metallurgist* **63**, 1313–1320. https://doi.org/10.1007/s11015-020-00953-6 (2020).
14. Pershin, I. M., Papush, E. G., Kukharova, T. V. & Utkin, V. A. Modeling of distributed control system for network of mineral water wells. *Water* **15**, 2289. https://doi.org/10.3390/w15122289 (2023).
15. Yao, L., Zhao, L., Fan, Q., Li, Y. & Mei, Q. Establishing the energy consumption prediction model of aluminum electrolysis process by genetically optimizing wavelet neural network. *Front. Energy Res.* **10**, 1009840. https://doi.org/10.3389/fenrg.2022.1009840 (2022).
16. Cicek, E. & Ozturk, K. Optimizing the artificial neural network parameters using a biased random key genetic algorithm for time series forecasting. *Appl. Soft Comput.* **10**, 107091 (2021).
17. Gui, W.-H., Yue, W.-C., Xie, Y.-F., Zhang, H.-L. & Yang, C.-H. A review of intelligent optimal manufacturing for aluminum reduction production. *Zidonghua Xuebao/Acta Autom. Sin.* **44**, 1957–1970 (2018).
18. Li, T.-F. *et al.* An improved UKFNN based on square root filter and strong tracking filter for dynamic evolutionary modeling of aluminum reduction cell. *Zidonghua Xuebao/Acta Autom. Sin.* **40**(3), 522–530. https://doi.org/10.3724/SP.J.1004.2014.00522 (2014).
19. Wang, Z.-B., Li, C.-M. & He, W.-Y. Control of alumina concentration in aluminum electrolysis production. *Nonferrous Metals Des.* **45**(2), 101–103 (2018).
20. Hu, H.-W. & Cao, X. Technology upgrading and application of high amperage aluminum reduction pots. *Light Metals* **5**, 18–21 (2017).
21. Guo, J., Gui, W.-H. & Wen, X.-H. Multi-objective optimization for aluminum electrolysis production process. *Zhongnan Daxue Xuebao (Ziran Kexue Ban)/J. Central South Univ. (Sci. Technol.)* **43**(2), 548–553 (2012).
22. Song, P., Zhao, C. & Huang, B. SFNet: A slow feature extraction network for parallel linear and nonlinear dynamic process monitoring. *Neurocomputing* **488**, 359–380. https://doi.org/10.1016/j.neucom.2022.03.012 (2022).
23. Marinina, O. *et al.* Technical and economic assessment of energy efficiency of electrification of hydrocarbon production facilities in underdeveloped areas. *Sustainability* **15**, 9614. https://doi.org/10.3390/su15129614 (2023).
24. Marinina, O., Kirsanova, N. & Nevskaya, M. Circular economy models in industry: Developing a conceptual framework. *Energies* **15**, 9376. https://doi.org/10.3390/en15249376 (2022).
25. Sidorenko, A. A., Dmitriev, P. N., Alekseev, V. Y. & Sidorenko, S. A. Improvement of techno-logical schemes of mining of coal seams prone to spontaneous combustion and rockbumps. *J. Min.Inst.* **15**, 1–13. https://doi.org/10.31897/PMI.2023.37 (2023).
26. Kazanin, O. I., Sidorenko, A. A., Sidorenko, S. A., Ivanov, V. V. & Mischo, H. High productive longwall mining of multiple gassy seams: Best practice and recommendations. *Acta Montan. Slovaca.* **27**, 152–162. https://doi.org/10.46544/AMS.v27i1.11 (2022).
27. Sidorenko, A. A., Sidorenko, S. A. & Ivanov, V. V. Numerical modelling of multiple-seam coal mining at the Taldinskaya-Zapadnaya-2 mine. *ARPN J. Eng. Appl. Sci.* **5**, 568–574 (2021).
28. Korshunov, G. I., Eremeeva, A. M. & Drebenstedt, C. Justification of the use of a vegetal additive to diesel fuel as a method of protecting underground personnel of coal mines from the impact of harmful emissions of diesel-hydraulic locomotives. *J. Min. Inst.* **247**(1), 39–47 (2021).
29. Pashkevich, M. A. & Kharko, P. A. The use of a composite mix to remove metals from acidic drainage waters at tailings facilities. *Obogashchenie Rud* **2022**(4), 40–47 (2022).
30. Kukharova, T. V., Ilyukhina, Y. A. & Shestopalov, M. Y. Development of a methodology for controlling the process of heating metal blanks in a methodical furnace. In *Proceedings of the 2022 Conference of Russian Young Researchers in Electrical and Electronic Engineering*, 718–721 (ElConRus 2022, 2022).
31. Martirosyan, A. V., Kukharova, T. V. & Fedorov, M. S. Research of the hydrogeological objects' connection peculiarities. In *Proceedings of 2021 4th International Conference on Control in Technical Systems, CTS 2021*, 34–38 (2021).
32. Quiroz Cabascango, V., Bazhin, V. Y., Martynov, A. S. & Pardo Ojeda, F. R. Automatic control system for thermal state of reverberatory furnaces in production of nickel alloys. *Metallurgist* **66**(1), 104–116 (2022).
33. Bazhin, V. Y. & Issa, B. Influence of heat treatment on the microstructure of steel coils of a heating tube furnace. *J. Min. Inst.* **249**(5), 393–400. https://doi.org/10.31897/PMI.2021.3.8 (2021).
34. Wilson, P., Saintier, N., Palin-Luc, T., Sudret, B. & Bergamo, S. Statistical study of the size and spatial distribution of defects in a cast aluminium alloy for the low fatigue life assessment. *Int. J. Fatigue* **166**, 107206. https://doi.org/10.1016/j.ijfatigue.2022.107206 (2022).
35. Mondolfo, L. F. *Aluminium Alloys, Structure and Propreties* (Butterworths, London, 1976).
36. Buffière, J.-Y., Savelli, S., Jouneau, P. H., Maire, E. & Fougères, R. Experimental study of porosity and its relation to fatigue mechanisms of model Al–Si7–Mg0.3 cast Al alloys. *Mater. Sci. Eng. A* **316**, 115–126 (2002).
37. McDowell, D. & Dunne, F. Microstructure-sensitive computational modeling of fatigue crack formation. *Int. J. Fatigue* **32**(9), 1521–1542. https://doi.org/10.1016/j.ijfatigue.2010.01.003 (2010).
38. Przybyla, C. P., Musinski, W. D., Castelluccio, G. M. & McDowell, D. L. Microstructure-sensitive HCF and VHCF simulations. *Int. J. Fatigue* **57**, 9–27. https://doi.org/10.1016/j.ijfatigue.2012.09.014 (2013).
39. Hor, A., Saintier, N., Robert, C., Palin-Luc, T. & Morel, F. Statistical assessment of multiaxial HCF criteria at the grain scale. *Int. J. Fatigue* **67**, 151–158. https://doi.org/10.1016/j.ijfatigue.2014.01.024 (2014).
40. Ben, A. A., Houria, M. I., Fathallah, R. & Sidhom, H. The effect of interacting defects on the HCF behavior of Al–Si–Mg aluminum alloys. *J. Alloys. Compd.* **779**, 618–629. https://doi.org/10.1016/j.jallcom.2018.11.282 (2019).
41. Khoukhi, D. *et al.* Probabilistic modeling of the size effect and scatter in high cycle fatigue using a Monte–Carlo approach: Role of the defect population in cast aluminum alloys. *Int. J. Fatigue* **147**, Article 106177. https://doi.org/10.1016/j.ijfatigue.2021.106177 (2021).
42. Khoukhi, D. *et al.* Spatial point pattern methodology for the study of pores 3D patterning in two casting aluminium alloys. *Mater. Charact.* **177**, Article 111165. https://doi.org/10.1016/j.matchar.2021.111165 (2021).
43. Katysheva, E. Analysis of the interconnected development potential of the oil, gas and transport industries in the Russian Arctic. *Energies* **16**, 3124. https://doi.org/10.3390/en16073124 (2023).
44. Katysheva, E. G. Application of BigData technology to improve the efficiency of Arctic shelf fields development. In *IOP Conference Series: Earth and Environmental Science*, Vol. 937 article 042080 (2021). https://doi.org/10.1088/1755-1315/937/4/042080.
45. Marinina, O., Tsvetkova, A., Vasilev, Y., Komendantova, N. & Parfenova, A. Evaluating the downstream development strategy of oil companies: The case of Rosneft. *Resources* **11**, 4. https://doi.org/10.3390/resources11010004 (2022).
46. Golovina, E., Khloponina, V., Tsiglianu, P. & Zhu, R. Organizational, economic and regulatory aspects of groundwater resources extraction by individuals (case of the Russian Federation). *Resources* **12**, 89 (2023).
47. Andreichyk, A. & Tsvetkov, P. Study of the relationship between economic growth and greenhouse gas emissions of the shanghai cooperation organization countries on the basis of the environmental Kuznets curve. *Resources* **12**(7), 80. https://doi.org/10.3390/resources12070080 (2023).
48. Buslaev, G., Lavrik, A., Lavrik, A. & Tcvetkov, P. Hybrid system of hydrogen generation by water electrolysis and methane partial oxidation. *Int. J. Hydrog. Energy* https://doi.org/10.1016/j.ijhydene.2023.03.098 (2023).

49. Golovina, E. & Shchelkonogova, O. Possibilities of using the unitization model in the development of transboundary groundwater deposits. *Water (Switzerland)* **15**(2), 298. https://doi.org/10.3390/w15020298 (2023).
50. Katysheva, E. Creation of the integrated field model to increase the oil and gas assets management. In *20th International Multidisciplinary Scientific GeoConference SGEM 2020.—18–24 August, 2020.—Volume 20. Ecology, Economics, Education and Legislation, Issue 5.2*, 153–160 (Environmental Economics, Albena, Bulgaria, 2020). https://doi.org/10.5593/sgem2020/5.2/s21.018.
51. Katysheva, E. G. The role of the Russian arctic gas industry in the northern sea route development. In *IOP Conference Series: Earth and Environmental Science*, Vol. 539 article 012075 (2020). https://doi.org/10.1088/1755-1315/539/1/012075
52. Marinin, M., Marinina, O. & Wolniak, R. Assessing of losses and dilution impact on the cost chain: Case study of gold ore deposits. *Sustainability* **13**, 3830. https://doi.org/10.3390/su13073830 (2021).
53. Golovina, E. I. & Grebneva, A. V. Features of groundwater resources management in the transboundary territories (on the example of the Kaliningrad region). *Geol. Miner. Resour. Sib.* **4**, 85–94 (2022).
54. Eremeeva, A. M., Kondrasheva, N. K., Khasanov, A. F. & Oleynik, I. L. Environmentally friendly diesel fuel obtained from vegetable raw materials and hydrocarbon crude. *Energies* https://doi.org/10.3390/en16052121 (2023).
55. Tarabarinova, T. A. & Golovina, E. I. Capitalization of mineral resources as an innovation ecological strategy. *Geol. Min. Res. Sib.* **4**, 86–96. https://doi.org/10.20403/2078-0575-2021-4-86-96 (2021).
56. Golovina, E. I. & Grebneva, A. V. Some aspects of groundwater resources management in transboundary areas. *J. Ecol. Eng.* **22**(4), 106–118. https://doi.org/10.12911/22998993/134037 (2021).
57. Pershin, I. M., Liashenko, A. L. & Papush, E. G. General principles for designing distributed control systems 2020 Wave Electronics and its Application in Information and Telecommunication Systems. *WECONF* **2020**, 9131485 (2020).
58. Martirosyan, A. V., Ilyushin, Yu. V. & Talanov N. A. Invention Patent № 2799233, publication date 04.07.2023, request № 2023107792/28 (30.03.2023), «Electromagnetic field diagnostic device».
59. Shapiro, S. L., Kopkov, M. P. & Potseshkovskaya, I. V. Problems of the organization of surface and underground space (e.g. historical embankments of Saint Petersburg). In *E3S Web of Conference*, Vol. 266 03016 (2021). https://doi.org/10.1051/e3sconf/202126603016.
60. Potseshkovskaya I. V. & Soroka, A. N. Revitalization of urban industrial areas based on sustainable development principles. In *E3S Web of Conference*, Vol. 266 08012 (2021). https://doi.org/10.1051/e3sconf/202126608012.
61. Demenkov, P. A., Trushko, O. V. & Potseshkovskaya, I. V. Numerical experiments on the modeling of compensatory injection for the protection of buildings during tunneling. *ARPN J. Eng. Appl. Sci.* **13**(23), 9161–9169 (2018).
62. Shubin, A. A., Tulin, P. K. & Potseshkovskaya, I. V. The mechanism of underground cavities formation and the methods of their elimination. *International Journal of Civil Engineering and Technology.* **8**(11), 667–681 (2017).
63. Sidorenko, A. A., Ivanov, V. V. & Sidorenko, S. A. Computer modeling of rock massif stress condition for mining planning on overworked seam. *J. Phys. Conf. Ser.* **1661**, 1–6. https://doi.org/10.1088/1742-6596/1661/1/012082 (2020).
64. Kazanin, O. I., Sidorenko, A. A., Meshkov, A. A. & Sidorenko, S. A. Reproduction of the longwall panels: Modern requirements for the technology and organization of the development operations at coal mines. *Eurasian Min.* **2**, 19–23 (2020).
65. Ignatenko A. & Afanaseva O. Application of system analysis methods for the research of mining enterprise activity. In *2023 Sixth International Conference of Women in Data Science at Prince Sultan University (WiDS PSU), Riyadh, Saudi Arabia*, 180–184 (2023). https://doi.org/10.1109/WiDS-PSU57071.2023.00045.
66. Meshkov, A. A., Korshunov, G. I., Kondrasheva, N. K., Eremeeva, A. M. & Seregin, A. S. Method of reducing air pollution of the coal mines working areas with diesel locomotives harmful emissions. *Bezopasnost' Truda v Promyshlennosti.* **1**, 68–72 (**In Russ**). https://doi.org/10.24000/0409-2961-2020-1-68-72 (2020).
67. Kondrasheva, N. K. Development of environmentally friendly diesel fuel. In *Petroleum Science and Technology* (eds Kondrasheva, N. K., Eremeeva, A. M., Nelkenbaum, K. S., Baulin, O. A. & Dubovikov, O. A.), **37**(12), 1478–1484 (2019). https://doi.org/10.1080/10916466.2019.1594285.
68. Korshunov, G. I., Eremeeva, A. M. & Seregin, A. S. Justification of reduction in air requirement in ventilation of coal roadways with running diesel engines. *MIAB Mining Inf. Anal. Bull.* **3**, 47–59 (**In Russ**). https://doi.org/10.25018/0236_1493_2022_3_0_47 (2022).
69. Kondrasheva, N. K., Eremeeva, A. M. & Nelkenbaum, K. S. Development of domestic technologies of producing high quality clean diesel fuel. *ChemChemTech [Izv. Vyssh. Uchebn. Zaved. Khim. Khim. Tekhnol.]* **61**(9–10), 76–82 (**in Russian**). https://doi.org/10.6060/ivkkt.20186109-10.5651 (2018).
70. Eremeeva, A. M., Ilyashenko, I. S. & Korshunov, G. I. The possibility of application of bioadditives to diesel fuel at mining enterprises. *MIAB Min. Inf. Anal. Bull.* **10–1**, 39–49. https://doi.org/10.25018/0236_1493_2022_101_0_39 (2022).
71. Afanaseva, O., Neyrus, S., Navatskaya, V. & Perezhogina, A. Risk assessment of investment projects using the simulation decomposition method. In *Fundamental and Applied Scientific Research in the Development of Agriculture in the Far East (AFE-2022). AFE 2023. Lecture Notes in Networks and System* Vol. 706 (eds Zokirjon-ugli, K. S. *et al.*) 776–785 (Springer, Cham, 2023). https://doi.org/10.1007/978-3-031-36960-5_88.
72. Zolotov O. I., Iliushina A. N. & Novozhilov I. M. spatially distributed system for monitoring of fields technical condition in mineral resources sector. In *2021 XXIV International Conference on Soft Computing and Measurements (SCM)*, 93–95 (St. Petersburg, Russia, 2021). https://doi.org/10.1109/SCM52931.2021.9507141.
73. Kovyazin, V. F., Nguyen, T. A. & Nguyen, T. T. Monitoring the forest fund lands of Kon Tum province, Vietnam using remote sensing data of Earth. *Geodesy. Cartogr.* **84**(8), 57–64 (**in Russian**). https://doi.org/10.22389/0016-7126-2023-998-8-57-64 (2023).
74. Bazhin, V. Y., *et al. IOP Conference Series: Materials Science and Engineering*, Vol. 862 032076 (2020). https://doi.org/10.1088/1757-899X/862/3/032076.
75. Iliushina A. N. and Novozhilov I. M., Development of the Spatial-Distributed Mathematical Model of a Drilling Rig, 2019 III International Conference on Control in Technical Systems (CTS), St. Petersburg, Russia, 2019, pp. 156–159. https://doi.org/10.1109/CTS48763.2019.8973298.
76. Trushnikov, V. E. *et al. IOP Conference Series: Materials Science and Engineering*, Vol. 760, 012062 (2020). https://doi.org/10.1088/1757-899X/760/1/012062.
77. Trushnikov, V. E. *et al. IOP Conference Series: Materials Science and Engineering*, Vol. 760 012063 (2020). https://doi.org/10.1088/1757-899X/760/1/012063.
78. Afanaseva, O., Bezyukov, O., Pervukhin, D. & Tukeev, D. Experimental study results processing method for the marine diesel engines vibration activity caused by the cylinder-piston group operations. *Inventions* **8**(3), 71. https://doi.org/10.3390/inventions8030071 (2023).
79. Arefiev, I. B. & Afanaseva, O. V. Implementation of control and forecasting problems of human-machine complexes on the basis of logic-reflexive modeling. In *Lecture Notes in Networks and Systemsthis, 2022, 442 LNNS*, 187–197 (2020). https://doi.org/10.1007/978-3-030-98832-6_17.
80. Afanaseva, O., Bezyukov, O., Pervukhin, D., Tukeev, D. Experimental Study Results Processing Method for the Marine Diesel Engines Vibration Activity Caused by the Cylinder-Piston Group Operations (2023) Inventions, 8 (3),71. https://doi.org/10.3390/inventions8030071

81. Plotnikov, A. V., Trushnikov, V. E., Pervukhin, D. A. & Shestopalov, M. Y. Mathematical simulation of the formation pressure monitoring system in the water-drive gas reservoir. In *Proceedings of 2023 26th International Conference on Soft Computing and Measurements, SCM 2023*, 77–81 (2023). https://doi.org/10.1109/SCM58628.2023.10159117.
82. Afanasev, P. M., Bezyukov, O. K., Ilyushina, A. N. & Pastukhova, E. V. Development of a system for controlling the temperature field of the columns and pipelines of raw gas transportation. *ARPN J. Eng. Appl. Sciencesthis* **18**(4), 421–434 (2023).
83. Iliushina A. N. , Shatilova N. A. & NovozhilovI. M. Development of the railroad switch electric drive mathematical model for the neural network. In *2023 XXVI International Conference on Soft Computing and Measurements (SCM)*, Saint Petersburg, Russian Federation, 64–68 (2023). https://doi.org/10.1109/SCM58628.2023.10159057.
84. Martynov, S. A. & Pervukhin, D. A. Algorithm for calculating of the carbon-graphite electrode consumption in an ore-thermal furnace and its position at different stages of smelting. In Chernye Metally, Vol. 5, 8–15 (2023). https://doi.org/10.17580/chm.2023.05.02.
85. Asadulagi, M. M.& Pervukhin, D. A. Stochastic control system of hydrodynamic processes in aquifers. In *Innovation-Based Development of the Mineral Resources Sector: Challenges and Prospects - 11th conference of the Russian-German Raw Materials, 2018*, 175–185 (2019).
86. Afanasyev, M., Pervukhin, D., Kotov, D., Davardoost, H. & Smolenchuk, A. System modeling in solving mineral complex logistic problems with the anylogic software environment. *Transp. Res. Procedia* **68**, 483–491. https://doi.org/10.1016/j.trpro.2023.02.065 (2022).
87. Bochkov, A., Pervukhin, D., Grafov, A. & Nikitina, V. Construction of Lorenz curves based on empirical distribution laws of economic indicators. *Math. Stat.* **8**(6), 637–644. https://doi.org/10.13189/ms.2020.080603 (2020).
88. Ilyushin, A. N., Kovalev, D. A. & Afanasev, P. M. Development of information measuring complex of distributed pulse control system. In: *2019 International Multi-Conference on Industrial Engineering and Modern Technologies*, FarEastCon 2019, 8934173 (2019). https://doi.org/10.1109/FarEastCon.2019.8934173.
89. Kivaev, I. N., Iliushina, A. N. & Novozhilov, I. M. Mathematical approach to the formalization of errors of operator's activities. In *Proceedings of 2018 17th Russian Scientific and Practical Conference on Planning and Teaching Engineering Staff for the Industrial and Economic Complex of the Region, PTES 2018*, Vol. 8604161, 106–107 (2019). https://doi.org/10.1109/PTES.2018.8604161.
90. Makarova A. A., Mantorova I. V., Kovalev D. A. & Kutovoy I. N. The modeling of mineral water fields data structure. In *IEEE Conference of Russian Young Researchers in Electrical and Electronic Engineering (ElConRus)*, 517–521 2021. https://doi.org/10.1109/ElConRus51938.2021.9396250.
91. Satsuk, T. P. *et al.* Erratum to: Automatic voltage stabilization of an electric rolling stock catenary system. *Russ. Electr. Engin.* **92**, 349. https://doi.org/10.3103/S1068371221300015 (2021).
92. Dagaev, A., Pham, V. D., Kirichek, R., Afanaseva, O. & Yakovleva, E. Method of analyzing the availability factor in a mesh network In *Communications in Computer and Information Science, 1552 CCIS*, 346–358 (2022). https://doi.org/10.1007/978-3-030-97110-6_27.
93. Kovalev D. A. & Rusinov L. A. Increase in environmental safety of recovery boiler. In *2022 IOP Conference Series: Earth and Environmental Science*, Vol. 990 012068. https://doi.org/10.1088/1755-1315/990/1/012068.
94. Zlotnikov, K. A., Afanaseva, O. V., Shestopalov, M. Y. & Skorobogaty, A. S. Enhancement of automated training systems for improvement of staff training quality. In *Proceedings of 2018 17th Russian Scientific and Practical Conference on Planning and Teaching Engineering Staff for the Industrial and Economic Complex of the Region, PTES 2018*, № 8604229, 33–35 (2019). https://doi.org/10.1109/PTES.2018.8604229.
95. Kukharova, T. V., Utkin, V. A. & Pershin, I. M. Modeling of a decision support system for a psychiatrist based on the dynamics of electrical conductivity parameters. In *Proceedings of the 2021 IEEE Conference of Russian Young Researchers in Electrical and Electronic Engineering, ElConRus 2021*, 975–978, 9396273 (2021). https://doi.org/10.1109/ElConRus51938.2021.9396273.
96. Pershin, I. M., Kukharova, T. V. & Tsapleva, V. V. Designing of distributed systems of hydrolithosphere processes parameters control for the efficient extraction of hydromineral raw materials. *J. Phys. Conf. Ser.* **1728**(1), 012017. https://doi.org/10.1088/1742-6596/1728/1/012017 (2021).
97. Pershin, I. M., Papush, E. G., Malkov, A. V., Kukharova, T. V. & Spivak, A. O. Operational control of underground water exploitation regimes. In *Proceedings of 2019 3rd International Conference on Control in Technical Systems, CTS 2019*, 77–80, 8973323 (2019). https://doi.org/10.1109/CTS48763.2019.8973323.
98. Asadulagi, M. M. The use of distributed and lumped type controllers for the hydro-lithospheric process control system of the kislovodskoye field. In *Proceedings of 2019 3rd International Conference on Control in Technical Systems, CTS 2019*, St. Petersburg, 30 октября – 01 2019 года (eds Asadulagi, M. M. & Vasilkov, O. S.) 7–10 (Institute of Electrical and Electronics Engineers Inc., St. Petersburg, 2019). https://doi.org/10.1109/CTS48763.2019.8973272.
99. Fetisov, V. *et al.* On the Integration of CO_2 capture technologies for an oil refinery. *Energies* **16**, 865. https://doi.org/10.3390/en16020865 (2023).
100. Fetisov, V., Shalygin, A. V., Modestova, S. A., Tyan, V. K. & Shao, C. Development of a Numerical Method for Calculating a Gas Supply System during a Period of Change in Thermal Loads. *Energies* **16**, 60. https://doi.org/10.3390/en16010060 (2023).
101. Schipachev, A., Fetisov, V., Nazyrov, A., Donghee, L. & Khamrakulov, A. Study of the pipeline in emergency operation and assessing the magnitude of the gas leak. *Energies* **15**, 5294. https://doi.org/10.3390/en15145294 (2022).
102. Nikolaev, A., Romanov, A., Zaripova, N. A., & Fetisov, V. G. Modeling of flow in field pipeline to confirm effectiveness of insertion of splitting couplings in control of rill-washing corrosion. In *IOP Conference Series: Earth and Environmental Science*, 194 (2018). https://doi.org/10.1088/1755-1315/194/8/082030.
103. Nikolaev, A., Samigullin, G. H., Samigullina, L. G. & Fetisov, V. G. Non-stationary operation of gas pipeline based on selections of travel. In *IOP Conference Series: Materials Science and Engineering*, 327 (2018). https://doi.org/10.1088/1757-899X/327/2/022074.
104. Gafur, S., Andrey, S., Liliya, S. & Vadim, F. Assessment of damage of metallic elements in oil and gas facilities using small punch test. *Int. J. Appl. Eng. Res.* **12**(21), 11583–11587 (2017).
105. Kukharova, T. V., Utkin, V. A. & Boev, I. V. Observation and prediction systems modeling for human mental state. In *2018 International Multi-Conference on Industrial Engineering and Modern Technologies*, 8602831 (FarEastCon 2018, 2018). https://doi.org/10.1109/FarEastCon.2018.8602831
106. Asadulagi, M. M. Synthesis of lumped and distributed controllers for control system of hydrodynamic process. In *2019 International Multi-Conference on Industrial Engineering and Modern Technologies, FarEastCon 2019, Vladivostok, 01–04 октября 2019 года* (eds Asadulagi, M. M., Ioskov, G. V. & Tronina, E. V.) 8933859 (Vladivostok: Institute of Electrical and Electronics Engineers Inc., 2019). https://doi.org/10.1109/FarEastCon.2019.8933859.
107. Embarcadero Technologies. https://community.embarcadero.com/
108. Github Markus MHumm. ComPortDriver. https://github.com/MHumm/ComPortDriver
109. Software Development Lohninger. http://www.lohninger.com/download.html
110. Ji, F., Hu, J. & Zhang, Y. Functionalized carbon-nanotubes-based thin-film transistor sensor for highly selective detection of methane at room temperature. *Chemosensors* **11**, 365. https://doi.org/10.3390/chemosensors11070365 (2023).
111. Sajovic, I., Kert, M. & Boh Podgornik, B. Smart textiles: A review and bibliometric mapping. *Appl. Sci.* **13**, 10489. https://doi.org/10.3390/app131810489 (2023).

112. Xie, L. *et al.* Pauling-type adsorption of O_2 induced electrocatalytic singlet oxygen production on N-CuO for organic pollutants degradation. *Nat. Commun.* **13**, 1–11 (2022).
113. Riente, P., Fianchini, M., Llanes, P., Pericas, M. A. & Noel, T. Shedding light on the nature of the catalytically active species in photocatalytic reactions using Bi_2O_3 semiconductor. *Nat. Commun.* **12**, 1–10 (2021).
114. Chen, X. *et al.* Photocatalytic removal of antibiotics by MOF-derived Ti3+-and oxygen vacancy-doped anatase/rutile TiO_2 distributed in a carbon matrix. *Chem. Eng. J.* **427**, Article 130945 (2022).
115. Liu, C. *et al.* Enhanced photocatalytic degradation performance of $BiVO_4$/BiOBr through combining Fermi level alteration and oxygen defect engineering. *Chem. Eng. J.* **449**, Article 137757 (2022).
116. Riemer, R., Nuckols, R. W. & Sawicki, G. S. Extracting electricity with exosuit braking. *Science* **372**, 909–911 (2021).
117. Li, J. *et al.* Enhancing photodegradation of methyl orange by coupling piezo-phototronic effect and localized surface plasmon resonance. *Nano Energy.* **108**, 108234. https://doi.org/10.1016/j.nanoen.2023.108234 (2023).
118. Wu, D. *et al.* Flexible, wearable multilayer piezoresistive sensor based on mulberry silk fabric for human movement and health detection. *J. Mater. Sci. Mater. Electron.* **34**, 1313. https://doi.org/10.1007/s10854-023-10691-5 (2023).
119. Zhang, R. *et al.* Sensitive and wearable carbon nanotubes/carbon black strain sensors with wide linear ranges for human motion monitoring. *J. Mater. Sci. Mater. Electron.* **29**, 5589–5596 (2018).
120. Ding, H. *et al.* Constructing conductive titanium carbide nanosheet (MXene) network on natural rubber foam framework for flexible strain sensor. *J. Mater. Sci. Mater. Electron.* **33**(19), 15563–15573 (2022).
121. Olivieri, F. *et al.* Reduced graphene oxide/polyurethane coatings for wash-durable wearable piezoresistive sensors. *Cellulose* https://doi.org/10.1007/s10570-023-05042-w (2023).
122. Altaf, M. *et al.* Ultrasensitive piezoresistive strain sensors based on CNTs/Ag-NPs coated highly stretchable textile. *J. Mater. Sci. Mater. Electron.* **31**, 9870–9877 (2020).
123. Litvinenko, V. S. *et al.* Assessment of the role of the state in the management of mineral resources. *J. Min. Inst.* https://doi.org/10.31897/PMI.2022.100 (2022).
124. Kondrasheva, N. K. & Eremeeva, A. M. Production of biodiesel fuel from vegetable raw materials. *J. Min. Inst.* https://doi.org/10.31897/PMI.2022.15 (2023).

Author contributions
All the materials (code) available via the link were developed by the authors.

Competing interests
The authors declare no competing interests.

Additional information
Correspondence and requests for materials should be addressed to A.M.

Reprints and permissions information is available at www.nature.com/reprints.

Publisher's note Springer Nature remains neutral with regard to jurisdictional claims in published maps and institutional affiliations.